29 October 1999

ELSEVIER

Chemical Physics Letters 312 (1999) 606–612

CHEMICAL PHYSICS LETTERS

www.elsevier.nl/locate/cplett

An adiabatic picture for electron transfer in mixed-valence systems [1]

Jianshu Cao *

Department of Chemistry, Massachusetts Institute of Technology, Cambridge, MA 01239, USA

Received 28 January 1999; in final form 21 June 1999

Abstract

An adiabatic picture is proposed to analyze short-time electronic coherence and dephasing in mixed-valence systems, which cannot be described by the Redfield equation or the golden-rule rate theory. In this picture, electronic coherence arises from Rabi oscillations between two adiabatic surfaces and decays as a result of inhomogeneous distributions and thermal fluctuations of Rabi frequencies. The initial preparation and wavepacket dynamics modulate Rabi oscillations and thus influence electronic coherence. Comparisons between exact numerical results and the prediction from the proposed theory verify the accuracy of the adiabatic approximation in describing the short-time electronic dynamics.

1. Introduction

Quantum coherence in electron transfer (ET) reveals the nature of condensed-phase quantum processes and hence has become a subject of recent experimental and theoretical studies. Oscillations in electronic dynamics have been observed in photosynthetic reaction centers and other ET systems and are believed to arise from vibrational coherence [1–3]. In the weak electronic coupling limit, non-equilibrium golden-rule rate formulae can be derived to analyze the role of wavepacket coherence and its initial preparation [4,5]. Recent experiments on photo-induced electron transfer in mixed-valence compounds have demonstrated oscillations in electronic populations on the femtosecond timescale [6]. Detailed path-integral simulations [7,8] suggest that such oscillations take place in ET systems with large electronic coupling constants and are sensitive to the initial preparation of the nuclear bath modes associated with the transfer processes.

As a function of the ratio between λ (the bath reorganization energy) and V (the electronic coupling constant), there is a transition in electronic dynamics from the localized regime to the delocalized regime [9–13]. (i) In the localized regime ($\lambda \gg V$), the large induced reorganization energy destroys electronic coherence; hence, population transfer is an incoherent rate process, which can be described by the non-interacting blip approximation or golden-rule rate in the non-adiabatic limit and by transition state theory in the adiabatic limit [14–16]. (ii) In the delocalized regime ($\lambda \leqslant V$), the electronic wavefunction extends to both the donor and acceptor states and electronic coherence persists over several

* E-mail: jianshu@mit.edu

[1] This Letter is dedicated to Professor Kent Wilson.

0009-2614/99/$ - see front matter
PII: S0009-2614(99)00840-4

oscillations [9]. It is these initial oscillations and their immediate decay that we will focus on in this Letter.

The electronic coupling constant of mixed-valence compounds is estimated to be in the range of 10^3 cm^{-1}, which is in the same order as the reorganization energy [1,8]. Because of the delocalization nature of electronic states, adiabatic surfaces are a simpler representation than localized diabatic surfaces. In the adiabatic picture, electronic coherence arises from Rabi oscillations between two adiabatic surfaces and decays because of electronic dephasing. Thus, initial preparation and wavepacket dynamics can modulate Rabi oscillations and the overall electronic dynamics. As demonstrated below, such an adiabatic picture can be useful for understanding fast electronic dynamics in strongly coupled systems.

2. Theory

The ET Hamiltonian can be written as

$$H_{\mathrm{ET}} = H_1(q)|1\rangle\langle 1| + H_2(q)|2\rangle \times\langle 2| + V(|1\rangle\langle 2| + |1\rangle\langle 2|), \quad (1)$$

where H_1 and H_2 are the diabatic Hamiltonians of donor and acceptor states, respectively, and V is the electronic coupling constant between the two diabatic states. The diabatic Hamiltonians are functions of a set of nuclear bath coordinates. Formally, if the quantity of interest is electronic dynamics, the donor state population can be expressed as

$$P_1(t) = \langle|\psi_1(t)|^2\rangle, \quad (2)$$

where the average is taken over all possible bath trajectories. Here, $\psi(t)$ is the solution to the time-dependent Schrödinger equation

$$\mathrm{i}\hbar\dot{\psi}(t) = H_{\mathrm{ET}}[q(t)]\psi(t), \quad (3)$$

for a given bath trajectory. For a Gaussian bath linearly coupled to electronic states, this formal expression forms the basis for the stochastic Gaussian bath method [17] and other related path-summation methods.

In this Letter, we seek a closed-form approximate solution to Eq. (2). Strongly mixed ET systems are characterized by electronic timescales much faster than nuclear timescales. Consequently, we can invoke the adiabatic approximation such that the solution to a constant two-level Hamiltonian is used to represent the electronic wavefunction, giving

$$|\psi_1(t)|^2 - |\psi_2(t)|^2 = \frac{1}{\omega(t)\,\omega(0)}\{U(t)U(0) + V^2\cos[\theta(t)]\} \quad (4)$$

with the initial condition $\psi_1(0) = 1$ and $\psi_2(0) = 0$. In Eq. (4), $U = (H_2 - H_1)/2$ is the potential difference between the two diabatic surfaces, $\omega = \sqrt{U^2 + V^2}$ is the instantaneous Rabi frequency, and $\theta(t) = 2\int_0^t \omega(t')\,\mathrm{d}t'$ is the phase difference between the two electronic states. Here, the time dependence in $U(t)$ and $\omega(t)$ arises implicitly from the functional dependence on the bath trajectory. For simplicity, the Planck constant $\hbar$ is assumed to be unity. This type of adiabatic approximation has been used to solve optical Bloch equations under slowly varying laser fields and is the working principle for population inversion by adiabatic frequency sweeping [18].

To proceed, we take the integration of the second-order time derivative of Eq. (4) so that

$$k(t) = -\frac{\mathrm{d}P_1(t)}{\mathrm{d}t} = 2V^2\Re\left\langle\int_0^t \mathrm{d}t'\frac{\omega(t')}{\omega(0)}\exp[\mathrm{i}\theta(t')]\right\rangle, \quad (5)$$

where $\Re$ denotes the real part of a complex function, the time-derivative is applied only to the phase factor θ, and the identity $\dot{P}_1(t) = -\dot{P}_2(t)$ is used. Next, the integral in Eq. (5) is factorized and approximated by the corresponding mean values, i.e.,

$$k(t) \approx 2V^2\Re\int_0^t \mathrm{d}t'\frac{\langle\omega(t')\rangle}{\langle\omega(0)\rangle}\langle\exp[\mathrm{i}\theta(t')]\rangle, \quad (6)$$

and the exponential part is truncated to second order in cumulant expansion, i.e.,

$$\langle\exp[\mathrm{i}\theta(t)]\rangle = \exp\left\{\mathrm{i}2\int_0^t\langle\omega(t_1)\rangle\,\mathrm{d}t_1 - 2\int_0^t\mathrm{d}t_1\int_0^t\mathrm{d}t_2 \times[\langle\omega(t_1)\omega(t_2)\rangle - \langle\omega(t_1)\rangle\langle\omega(t_2)\rangle]\right\}. \quad (7)$$

Further, nuclear trajectories are represented by the

mean $\bar{q}(t)$ and the deviation from the mean $\delta q(t)$, i.e., $q(t) = \bar{q}(t) + \delta q(t)$. On expanding the exponent to second order in δq, we have

$$\langle \exp[\mathrm{i}\theta(t)] \rangle = \exp\left\{ \mathrm{i}2\int_0^t \langle \omega(t_1) \rangle \, \mathrm{d}t_1 - \int_0^t \int_0^{t_1} \eta(t_1) \times \eta(t_2) C(t_1,t_2) \, \mathrm{d}t_1 \, \mathrm{d}t_2 \right\}, \quad (8)$$

where the coefficient $\eta(t)$ is defined as $\eta(t) = 2\partial\omega[\bar{q}(t)]/\partial\bar{q}(t)$ and the time-correlation function is defined as $C(t_1,t_2) = \langle \delta q(t_1) \delta q(t_2) \rangle - \langle \delta q(t_1) \rangle \langle \delta q(t_2) \rangle$. To be consistent, the time-dependent frequency is also truncated to second order in δq, giving

$$\langle \omega(t) \rangle = \langle \omega[q(t)] \rangle \approx \omega[\bar{q}(t)] + \tfrac{1}{2} \frac{\partial^2 \omega[\bar{q}(t)]}{\partial \bar{q}(t)^2} C(t,t) . \quad (9)$$

Then, for a given $\bar{q}(t)$ and $C(t_1,t_2)$, the evolution of electronic population $P_1(t)$ or $P_2(t)$ can be explicitly computed from Eqs. (6) and (8).

The adiabatic approximation in Eq. (4) ignores transitions between the two adiabatic surfaces, under the conditions of strong electronic mixing and weak nuclear dissipation. The resulting expression in Eq. (6) predicts the initial behavior of electron coherence but fails to recover long-time rate behavior, especially for a fast bath and large bath fluctuations. In comparison, the well-known non-interacting blip approximation [13] or the Redfield theory [10] leads to a convoluted rate expression: $P(t) = -\int_0^t K(t-\tau) P(\tau) \, \mathrm{d}\tau$, where $k_{gr} = \int_0^\infty K(t)$ is the golden-rule rate. Such a convolution relation can be derived from the diabatic representation and is valid if the electronic coupling is relatively weak or the nuclear correlation time is relatively short [19]. At very short-times, the convolution term in the Redfield equation may lead to unphysical results. Therefore, the adiabatic representation introduced here provides a unique framework to analyze the electronic coherent regime, which has not been described by other ET theories.

To further examine the adiabatic picture, we make the following observations:

1. Taking the second-order derivative of Eq. (4) is intended to minimize the inhomogeneous effect on the prefactor, so that for an adiabatic bath Eq. (6) becomes exact. The steps leading to Eqs. (6) and (8) from Eq. (8) involve the factorization in Eq. (6) and the cumulant expansion in Eq. (8). By incorporating higher-order correlations, we can systematically improve the accuracy of there approximations.
2. For a stationary bath, the correlation function is time-invariant, i.e., $C(t_1,t_2) = C(t_1 - t_2)$. Then, in Eq. (8), the time-dependence in $C(t)$ is determined by the intrinsic nature of solvent fluctuations, whereas the time-dependence in $\langle \omega(t) \rangle$ reflects the wavepacket motions arising from the non-equilibrium initial preparation. Within the linear response regime, the central frequency relaxation, $\langle \omega(t) \rangle$, and the solvent correlation function, $C(t)$, is related through fluctuation–dissipation theory, which in the classical limit can be expressed as $\langle \omega(t) \rangle / \langle \omega(0) \rangle = C(t)/C(0)$.
3. The above analysis holds for both classical and quantum baths. For a quantum bath, the complex time-correlation function satisfies the detailed balance relationship; hence, the ET system will approach thermal equilibrium asymptotically. For a classical bath, the time-correlation function does not guarantee energy conservation between the bath and the ET system. Since the short-time behavior is the focus of this Letter, the inconsistency of mixed classical-quantum dynamics is not a major concern for our purpose.
4. In the nonadiabatic golden-rule limit, the electronic coupling function V is much smaller than the potential difference U such that $\omega \approx U$. Then, Eq. (5) is reduced to

$$k(t) = 2V^2 \Re \int_0^t \mathrm{d}t' \left\langle \exp\left\{ -\mathrm{i}\int_0^{t'} U[q(t_1)] \, \mathrm{d}t_1 \right\} \right\rangle, \quad (10)$$

which is exactly the golden-rule expression derived from first-order perturbation theory. [16]

5. For white noise, the Redfield equation or the non-interacting blip approximation can be reduced to the Bloch equation, which is valid in the strong electronic coupling regime. However, ET

processes take place with correlated solvent fluctuations or even inhomogeneous environments as assumed in the Marcus model, because white noise does not localize electronic states.

3. Results and discussions

The general theory presented in the previous section makes no assumptions about the specific form of electronic surfaces. As an illustrative example, we use the Gaussian bath Hamiltonian

$$H_{\mathrm{ET}} = H_{\mathrm{b}}(E)(|1\rangle\langle 1| + |2\rangle\langle 2|) + (\varepsilon + \lambda - E)|2\rangle\langle 2| + V(|1\rangle\langle 2| + |1\rangle\langle 2|), \tag{11}$$

where H_{b} is the Gaussian bath Hamiltonian, ε is the free energy difference between the donor and acceptor states, λ is the reorganization energy, and E is the solvent polarization energy defined with respect to the equilibrium bath distribution at the donor state. Here, the bath variable $E(t)$ represents the collective effect of the bath and is equivalent to the variable q in Eq. (1). This ET Hamiltonian is better known as the spin-boson model or the Brownian oscillator model.

On applying Eqs. (6) and (8) to the Gaussian bath Hamiltonian, we obtain

$$k = 2V^2\Re\int_0^t \mathrm{d}t' \frac{\langle\omega(t')\rangle}{\langle\omega(0)\rangle} \times \exp\left\{\mathrm{i}2\int_0^{t'}\langle\omega(t_1)\rangle\,\mathrm{d}t_1 - \int_0^{t'}\int_0^{t_1}\eta(t_1) \times \eta(t_2)C(t_2 - t_1)\,\mathrm{d}t_1\,\mathrm{d}t_2\right\}, \tag{12}$$

where the adiabatic frequency is given as

$$\omega = \sqrt{V^2 + \frac{[\varepsilon + \lambda - E]^2}{4}}\,, \tag{13}$$

the mean frequency is given by Eq. (9) as

$$\langle\omega(t)\rangle \approx \bar{\omega}(t) + \frac{[1 - \eta^2(t)]}{8\omega(t)}C(0), \tag{14}$$

with $\bar{\omega}(t) = \omega[\bar{E}(t)]$, and $\eta(t)$ is given as

$$\eta(t) = \frac{\varepsilon + \lambda - \bar{E}(t)}{2\omega(t)}. \tag{15}$$

As before, we define the polarization energy as $E(t) = \bar{E}_p(t) + \delta E(t)$ and hence the bath correlation function as $C(t) = \langle\delta E(t)\delta E(0)\rangle$, which can be explicitly expressed in terms of the spectrum density defined in the spin-boson model [20].

The formulation in this Letter holds for both classical and quantum baths; however, for simplicity, numerical examples are given only for classical Gaussian baths. Unless specified, the parameters in Eq. (11) take the value of $\beta\lambda = 40$, $\beta\delta = 20$, and $\beta\varepsilon = 0$. To verify the accuracy of the adiabatic approximation, we obtain exact results via a numerical path summation method, in which bath trajectories are sampled from the bath Hamiltonian, the electronic wavefunction is solved from Eq. (3) for a given trajectory, and electronic dynamics is computed by averaging the wavefunction over the bath trajectories as in Eq. (2) [17].

3.1. Adiabatic bath: inhomogeneous dephasing

The classical rate in Marcus ET theory is derived under the assumption of an adiabatic bath [14,15]. An adiabatic Gaussian bath has an infinitely long correlation with only zero-frequency fluctuations. Thus, the time-dependent expression in Eq. (6) can be simplified to

$$k(t) = 2V^2\Re\int_0^t \mathrm{d}t' \exp\left\{2\mathrm{i}\langle\omega\rangle t' - \eta^2\lambda t'^2/\beta\right\}, \tag{16}$$

where $C(t) = 2\lambda/\beta$. In this case, the adiabatic approximation in Eq. (4) is exact and Rabi oscillations, which dominate the initial electronic dynamics, decay because of the inhomogeneous distribution of Rabi frequencies. The asymptotic limit of Eq. (16) is

$$\lim_{t\to\infty} k(t) = V^2\sqrt{\frac{\pi\beta}{\eta^2\lambda}}\exp - \left\{\frac{\beta}{4\lambda}\left[(\lambda + \varepsilon) + \frac{4V^2}{\lambda + \varepsilon}\right]^2\right\}, \tag{17}$$

which has the same form as the Marcus ET rate except that the activation energy depends on electronic coupling.

For an adiabatic Gaussian bath, the diabatic Hamiltonians in Eq. (1) are explicitly given as $H_1 = E^2/(4\lambda)$ and $H_2 = E^2/(4\lambda) + \varepsilon - E + \lambda$, which defines the Marcus parabolic curves. The adiabatic surfaces are obtained by diagonalizing the diabatic Hamiltonian. In Fig. 1, adiabatic and diabatic surfaces are plotted for $\beta\lambda = 40$, $\beta V = 20$, and $\beta\varepsilon = 0$, which, as described in Section 1, corresponds to a transition between localization and delocalization.

The usual initial preparation is $E(0) = 0$, which is the equilibrium configuration of the donor states. For an adiabatic bath, non-equilibrium distributions are equivalent to a re-definition of ε through $\varepsilon' = \varepsilon - E(0)$. A barrierless ET with $\varepsilon = 0$ or equivalently a non-equilibrium bath with $E(0) = \lambda$ has the largest oscillation amplitude and hence the strongest electronic coherence.

In Fig. 2, electronic populations on the donor state are plotted for $\beta V = 20$ and $\beta V = 5$, respectively. The unit of time is scaled at room temperature $T = 300$ K. As shown in Fig. 2, the oscillation amplitude and frequency increase with the electronic coupling constant. Further, because of the broad distribution of Rabi frequencies, the initial oscillations are dissipated by inhomogeneous dephasing. At both electronic coupling constants, the result calcu-

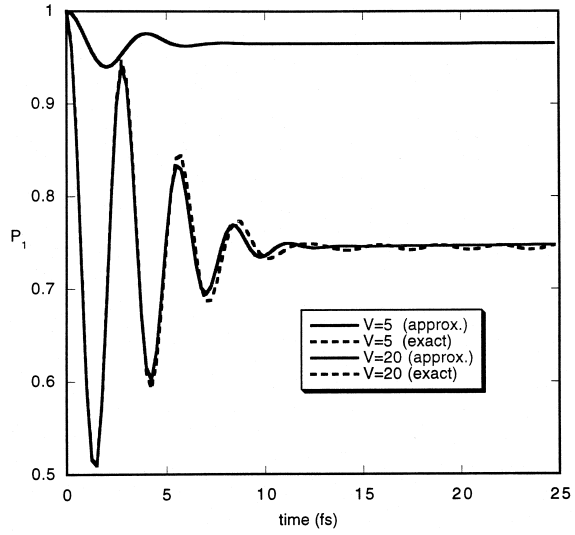

Fig. 2. Donor state population $P_1(t)$ for an adiabatic bath with $\beta V = 5$ (upper curves) and $\beta V = 20$ (lower curves), respectively. The energy and time units are scaled by room temperature $T = 300$ K. The bath is prepared from thermal equilibrium at the donor state. The solid curves are evaluated from Eq. (16) and the dotted curves are obtained by path-summation simulations.

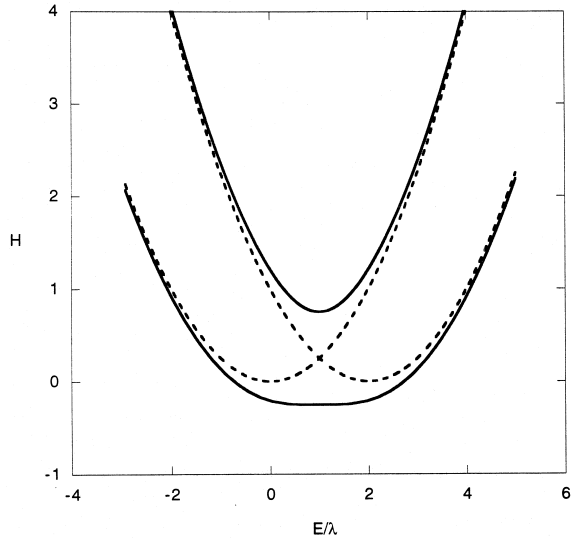

Fig. 1. Adiabatic potential surfaces (solid curves) versus diabatic potential surfaces (dotted curves). The diabatic Hamiltonians are $H_1(E) = E^2/(4\lambda)$ for the donor state and $H_2(E) = E^2/(4\lambda) + \lambda - E$ for the acceptor state, with reorganization energy $\beta\lambda = 40$ and electronic coupling $\beta V = 20$.

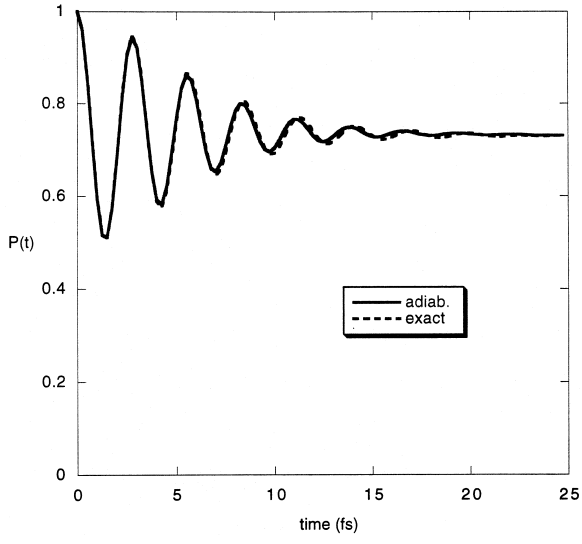

Fig. 3. Donor state population $P_1(t)$ for a dynamic bath with $\beta\lambda = 40$ and with $\beta V = 20$. The bath correlation function is exponential $C(t) = \exp(-\gamma t)$ with $\beta\gamma = 5$. The solid curve is evaluated from Eq. (12) and the dotted curve is obtained by path-summation simulations.

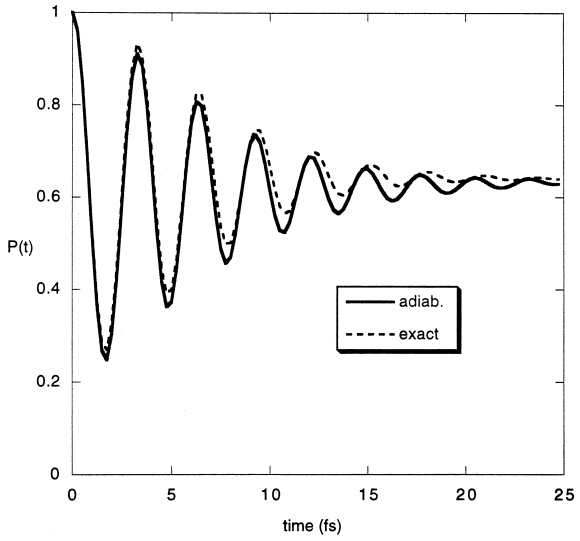

Fig. 4. The same plot as Fig. 3 except for the initial bath configuration at $E(0) = 0.5\lambda$ instead of at thermal equilibrium.

lated by the adiabatic approximation in Eq. (17) agrees well with the exact simulation results.

3.2. Dynamic bath: homogeneous dephasing

To incorporate nuclear dynamics, we assume an exponential decay correlation function, $C(t) = \exp(-\gamma t)C(0)$, with γ being the decay constant and $C(0) = 2\lambda/\beta$. The exponential decay describes a Debye dielectric solvent or an over-damped oscillator. The adiabatic limit is recovered by taking $\gamma = 0$ and the Markovian limit is recovered by taking $\gamma = \infty$. The dissipative electronic dynamics of a Markovian bath can be described by the Redfield equation and does not lead to a thermal activated rate process.

In Fig. 3, the donor state population is plotted as a function of time for $\beta\gamma = 5$. Again, the adiabatic approximation is verified by the numerical results. In comparison with the adiabatic bath in Fig. 2, the dynamics of the bath significantly enhances electronic coherence.

For a dynamic bath, the effect of the initial preparation is reflected both in the shift of the central frequency through $\overline{\omega}$ and in the modulation of the dephasing strength η. In Fig. 4, the donor state population is plotted as a function of time for the same system as in Fig. 3, but with a non-equilibrium configuration $E(0) = 0.5\lambda$. In comparison with Fig. 3, the initial oscillations become more dramatic because of the non-equilibrium preparation.

4. Concluding remarks

The nature of the proposed adiabatic approximation is electronic dephasing between adiabatic surfaces and nuclear dynamics on diabatic surfaces. At longer times, the adiabatic approximation starts to fail because of infrequent transitions between the adiabatic surfaces. Since the short-time electronic dynamics is of major interest to us, the adiabatic theory provides a simple physical picture for strongly coupled mixed-valence ET systems as well as a simple analytical method to model fast electron dynamics initiated by laser pulses. Recent studies using kinetic spectra [21] and non-adiabatic steepest descent paths [22] have demonstrated evidence to support the adiabatic picture. In the future, the proposed method will be compared with other theories to examine the validity of each approach.

Acknowledgements

This work is supported by the MIT start-up fund and by the Donors of the Petroleum Research Fund administrated by the American Chemical Society. The author thanks David Reichman for communicating similar views on the subject and an anonymous reviewer for insightful comments.

References

[1] M.H. Vos, F. Rappaport, J.-C. Lambry, J. Breton, J.-L. Martin, Nature 363 (1993) 320.
[2] D. Jonas, S. Bradford, S. Passino, G. Fleming, J. Chem. Phys. 99 (1995) 2554.
[3] D.C. Arnett, P. Vohringer, N.F. Scherer, J. Am. Chem. Soc. 117 (1995) 12262.
[4] R.D. Coalson, D.G. Evans, A. Nitzan, J. Chem. Phys. 101 (1994) 486.
[5] M. Cho, R.J. Silbey, J. Chem. Phys. 103 (1995) 595.
[6] P.J. Reid, C. Silva, P.F. Barbara, L. Karki, J.T. Hupp, J. Chem. Phys. 99 (1995) 2609.

[7] A. Lucke, C.H. Mak, R. Egger, J. Ankerhold, J. Stockburger, H. Grabert, J. Chem. Phys. 107 (1997) 8397.
[8] D.G. Evans, A. Nitzan, M.A. Ratner, J. Chem. Phys. 108 (1997) 6387.
[9] R.A. Harris, R. Silbey, J. Chem. Phys. 78 (1983) 7330.
[10] R. Silbey, R.A. Harris, J. Chem. Phys. 80 (1984) 2615.
[11] B. Carmeli, D. Chandler, J. Chem. Phys. 82 (1985) 3401.
[12] D. Chandler, in: D. Levesque, J. Hansen, J. Zinn-Justin (Eds.), Liquides, Cristallisation et Transition Vitreuse, Les Houches, Session LI, Elsevier, New York, 1991.
[13] A.J. Leggett, S. Chakravarty, A.T. Dorsey, M.P.A. Fisher, A. Garg, W. Zwerger, Rev. Mod. Phys. 59 (1987) 1.
[14] R.A. Marcus, N. Sutin, Biochim. Biophys. Acta. 811 (1985) 265.
[15] M.D. Newton, N. Sutin, Annu. Rev. Phys. Chem. 35 (1984) 437.
[16] J.S. Bader, R.A. Kuharski, D. Chandler, J. Chem. Phys. 93 (1990) 230.
[17] J. Cao, L.W. Ungar, G.A. Voth, J. Chem. Phys. 104 (1996) 4189.
[18] L. Allen, J.H. Eberly, Optical Resonance and Two-Level Atoms, Dover, New York, 1987.
[19] J. Cao, J. Chem. Phys. 107 (1997) 3204.
[20] A. Warshel, W.W. Parson, Ann. Rev. Phys. Chem. 42 (1991) 279.
[21] Y. Jung, R.J. Silbey, J. Cao, J. Phys. Chem., to be published.
[22] J. Cao, J. Chem. Phys. to be published.